Physica C 326–327 (1999) 63–71

Josephson phenomenology and microstructure of YBaCuO artificial grain boundaries characterized by misalignment of the *c*-axes

F. Tafuri [a,b,*], F. Miletto Granozio [a], F. Carillo [a], F. Lombardi [a], U. Scotti Di Uccio [a], K. Verbist [c], O. Lebedev [c], G. Van Tendeloo [c]

[a] *I.N.F.M.-Dip. Scienze Fisiche dell'Università di Napoli Federico II, P. le Tecchio 80, Naples, Italy*
[b] *Dip. Ingegneria dell'Informazione, Seconda Università di Napoli, Aversa (CE), Italy*
[c] *EMAT, University of Antwerp (RUCA), Groenenborgerlaan 171, B-2020 Antwerp, Belgium*

Received 25 April 1999; accepted 26 June 1999

Abstract

$YBa_2Cu_3O_{7-\delta}$ (YBCO) grain boundaries characterized by a misalignment of the *c*-axes (45° *c*-axis tilt or 45° *c*-axis twist) have been obtained by employing a recently implemented biepitaxial technique. Junctions based on these grain boundaries exhibit good Josephson properties useful for applications. High values of the $I_C R_N$ product and a Fraunhofer-like dependence of the critical current on the magnetic field, differently from traditional biepitaxial junctions, have been obtained. The correlation between transport properties and microstructure has been investigated by Transmission Electron Microscopy (TEM), which was also performed on previously measured junctions. The presence of atomically clean basal plane (BP) faced tilt boundaries, among other types of interfaces, has been shown. The possibility of selecting these kinds of boundaries by controlling film growth, and their possible advantages in terms of reproducibility and uniformity of the junction properties are discussed. The possibility of employing these junctions to explore the symmetry of the order parameter is also discussed.

PACS: 74.50 + r; 74.72Bk; 74.76.Bz; 74.80.Fp
Keywords: Josephson phenomenology; Microstructure; YBaCuO

1. Introduction

Grain boundary (GB) Josephson junctions (JJ) are considered fundamental both for the basic understanding of the nature of high critical temperature superconductors (HTS) and for the implementation of reliable technologies based on JJ. $YBa_2Cu_3O_{7-\delta}$ (YBCO) artificial grain boundaries (AGB) junctions have been for instance widely employed to investigate the order parameter symmetry in HTS [1–3]. Reproducible and high quality devices are routinely fabricated [4], although the desired clean homogeneous interface across the whole section of the microbridge has not been achieved by any of the known AGB fabrication technologies and the influ-

* Corresponding author. I.N.F.M.-Dip. Scienze Fisiche dell'Università di Napoli Federico II, P. le Tecchio 80, Naples, Italy. Tel.: +0039-81-76-82-584; fax: +0039-81-23-9-1821; E-mail: tafuri@axpna1.na.infn.it

PII: S0921-4534(99)00372-X

ence of GB microstructure on the transport properties is not completely understood. A detailed investigation of the relation between microstructure and transport properties is therefore highly desired both for a correct interpretation of experimental results and for the establishment of a technology able to provide reliable junctions for superconducting electronics. The most widely employed junctions are based on the bicrystal technique and are mainly characterized by a tilt in the *a–b* plane (i.e., a rotation around the *c*-axis) [5,6]. This type of GB, characterized by an in-plane rotation, can also be fabricated by the biepitaxial technique, where a seed layer is used to modify the YBCO crystal orientation on part of the substrate. This results in an artificial asymmetric 45° tilt in-plane GB [7]. The versatility of the biepitaxial technique is a key point in view of possible applications especially concerning the integration on small and large scale. On the other hand, the nature of GBs seems to be an intrinsic limit for real applications for this type of structure. A convincing explanation of this limitation has been given in terms of the d-wave nature of the order parameter and, in particular, by the presence of π-junctions at the junction interface [8]. As demonstrated by studies on bicrystals, based on the same type of 45° in-plane tilt GB, the presence of π-junctions reduces the $I_C R_N$ values (where I_C and R_N are the critical current and the high normal state resistance, respectively), prevents from obtaining a Fraunhofer-like magnetic pattern of I_C and determines unquantized flux noise at the GB [8].

YBCO junctions based on AGBs characterized by a 45° relative misalignment of the *c*-axes have been recently realized by employing a biepitaxial technique [9]. The AGB is obtained at the interface between a (103) film deposited over a (110) $SrTiO_3$ substrate and a (001) film deposited over a MgO seed layer (Fig. 1). Junctions associated with this AGB exhibit promising Josephson properties. Two different AGBs characterized by a 45° tilt or twist of the *c*-axis across the GB are considered. We will refer to them in the following as tilt or *twist* AGBs, respectively.

The aim of the present work is to investigate some, almost unexplored, configurations of the wide class of GBs characterized by a misalignment of the *c*-axes, looking for a direct correlation between GB microstructure and superconducting properties. This could be helpful in understanding the nature of transport in superconducting GBs. It is achieved by performing transport measurements on different types of junctions and by investigating the microstructure through Transmission Electron Microscopy (TEM). In particular, TEM analysis was also performed on samples whose transport properties were previously characterized. Such studies are of high technical difficulty since conventional cross section (CS) TEM

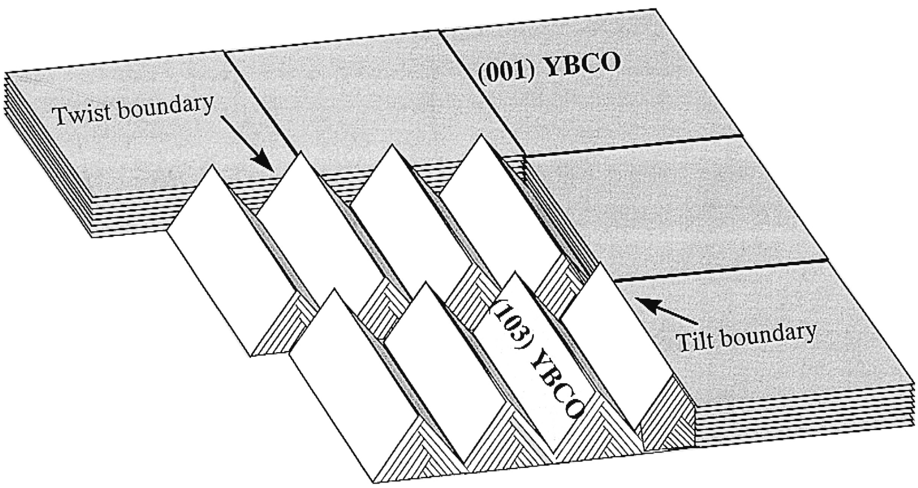

Fig. 1. A schematic representation of the AGB structure. The boundary is obtained at the interface between the (001) oriented YBCO film grown on the (110) MgO seed layer and the (103) YBCO film grown on the bare (110) STO substrate.

preparation of such a small specific region is extremely difficult [10].

It is demonstrated that the anisotropic and easily tunable properties of the proposed structure offer the possibility to investigate the influence of order parameter symmetry on the transport properties of AGBs, being somehow complementary with respect to that provided by bicrystals [1–3]. Finally, we will show that the technology we implemented provides a Josephson structure able to offer some advantages, in terms of applications, over junctions obtained by other techniques. Besides the ease of integration for circuit design, some examples are given by the obtained high values of the $I_C R_N$ product and Fraunhofer-like dependence of I_C on the magnetic field, which is fundamental for applications such as vortex flow transistors.

2. Junction fabrication procedure and experimental set-up

The fabrication process mainly involves the deposition of MgO and YBCO thin films and ion-milling procedures and has been reported in detail elsewhere [9,11,12]. (110) oriented MgO thin films (thickness 20 nm) are deposited by RF magnetron sputtering from a stoichiometric oxide target on (110) $SrTiO_3$ (STO) substrates at a substrate temperature of 600°C. A standard lithographic procedure, employing a Nb or photoresist mask and ion milling, was used to pattern the seed layer. $YBa_2Cu_3O_{7-x}$ films with a thickness of 120 nm were deposited by inverted cylindrical magnetron sputtering in an Ar/O_2 atmosphere ($P_{O_2} = P_{Ar} = 50$ Pa) at a temperature of 780°C. Finally, the final microbridge geometry was defined by ion milling keeping the sample holder at a temperature of −100°C. The milling procedure has been previously optimized in order not to decrease the critical temperature and current in (001) and (103) oriented microbridges a few μm wide.

The feasibility of a complementary technique, based on the deposition of a STO (110) buffer layer on a (110) MgO substrate has been also recently demonstrated, and is currently under investigation.

CS as well as plan view (PV) samples for electron microscopy have been prepared by standard mechanical polishing and ion milling. High resolution electron microscopy (HREM) observations were performed in a Jeol 4000 EX microscope with a point resolution of 0.17 nm. After the transport measurements some samples have been processed to be investigated by HREM. To this aim, a special procedure has been used, in which a focused ion beam thinning technique (FIB) creates an electron transparent region at the desired location on the sample. In combination with precision mechanical polishing typical of traditional TEM preparation, FIB allows us to prepare a CS TEM specimen at a very specific site (submicrometer range). Details can be found elsewhere [10].

3. Experimental results

The CS HREM investigations for the tilt and the twist case have been reported previously [9,10,13]. The expected 'ideal' structures for both AGBs have been found as well as other AGB configurations. In this paper, we will mainly focus on the microstructure of the tilt case. An example of tilt GB is given in Fig. 2, where a highly perfect faceted interface separates the (001) BP of the (103) oriented film and the (103) plane of the (001) film. This represents an optimal situation since an atomically clean structure can be obtained. For the case of tilt AGBs we have observed another kind of interface planes, as shown in Fig. 3. The tilt AGB exhibits an irregularly stepped interface. The orientation of the (103) domains at the interface is different in Figs. 2 and 3. The interface in Fig. 3 does not show any clear geometrical relation with the YBCO axes of either crystal. A qualita-

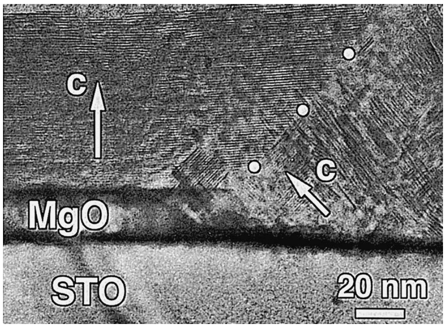

Fig. 2. CS TEM image of a 45° tilt AGB recorded along the $[001]_{STO}$ direction. The atomically flat AGB interface, following the basal plane (BP) face of the (103) film, is marked by dots.

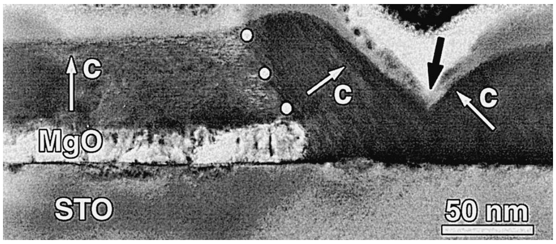

Fig. 3. CS TEM image of a 45° tilt AGB recorded along the $[001]_{STO}$ direction. The tilt AGB exhibits an irregularly stepped interface. This TEM analysis has been performed on a microbridge previously characterized in terms of its transport properties and therefore the sample has been prepared thorough the FIB technique.

tive model explaining the different morphologies of the tilt AGB shown in Figs. 2 and 3 is presented in Section 4.

In Fig. 4 the typical I–V characteristics at $T = 4.2$ K of a *twist* and a tilt junction are shown. One can clearly distinguish two different regimes in terms of the critical current densities J_C and the normal state specific conductances σ_N, corresponding to the two types of AGBs. Both the characteristics present a shape typical of the Resistively Shunted Junction (RSJ) model, but the junction characterized by the lower critical current density (i.e., tilt AGB) does not exhibit any excess current. Deviations from the RSJ model are more remarkable as the critical current density increases and therefore typically for the twist case. In both cases, the maximum working temperature T_C of the devices is typically higher than 77 K. *Twist* AGB junctions typically have J_C values in the range $0.1–4.0 \times 10^5$ A/cm^2 and σ_N values in the range 20–120 $(\mu\Omega\ \mathrm{cm}^2)^{-1}$ at $T = 4.2$ K. tilt AGB junctions have lower J_C and higher σ_N values, in the ranges $0.5–10 \times 10^3$ A/cm^2 and 1–10 $(\mu\Omega\ \mathrm{cm}^2)^{-1}$, respectively. J_C and σ_N values fall in the ranges typical for in-plane GB JJ, usually fabricated using bicrystal or conventional biepitaxial techniques [4]. The $I_C R_N$ values are high in both cases, of the order of 1–2 mV at $T = 4.2$ K and 50–100 μV at $T = 77$ K, respectively. These are plotted as a function of J_C and compared with those from other types of junctions [14] in Fig. 5. They are larger for the corresponding J_C values than those provided by conventional biepitaxials and are of the same order of magnitude as in bicrystal and step edge junctions. We also notice that the $I_C R_N$ does not seem to scale with the critical current density, differently from other types of junctions [14].

The current vs. voltage characteristics corresponding to the junction based on the AGB of Fig. 3 are shown at different temperatures in Fig. 6. The sample for TEM investigation was prepared by employing the FIB technique [10]. The critical current density is in this case 5×10^3 A/cm^2 as expected for this type of junction. From the temperature dependence of I vs. V curves, we can suppose the presence of two junctions in series, manifested in a typical shift due to the temperature of the step structure at high voltages. This behavior has been rarely observed in our junctions. Such a feature could be partly interpreted by observing the microstructure of Fig. 3. The (103) growth determines in this case a particularly thin region in proximity of the AGB, to which a reduction of the critical current

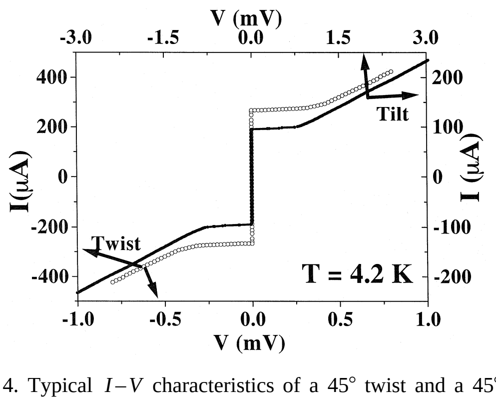

Fig. 4. Typical I–V characteristics of a 45° twist and a 45° tilt junction, measured at $T = 4.2$ K.

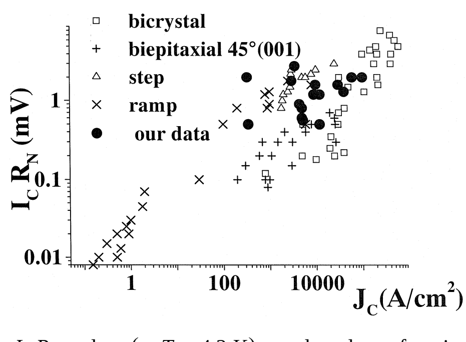

Fig. 5. $I_C R_N$ values (at $T = 4.2$ K) are plotted as a function of J_C and compared with those relative to other types of junctions.

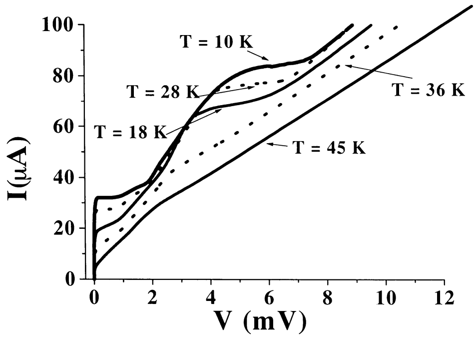

Fig. 6. The current vs. voltage characteristics corresponding to the junction based on the AGB of Fig. 3 are shown at different temperatures ($T = 10$, 18, 28, 36 and 45 K).

corresponds. In particular circumstances such a microbridge can dominate the electronic transport properties within a proper range. The TEM-FIB investigation allows in this case to determine the type of AGB generating the Josephson behavior, and eventually to study the correlation between anomalous effects in I vs. V characteristics and microstructure.

Differences between the tilt and twist cases are also evident in the dependence of the critical current I_C on the temperature T. In Fig. 7, the I_C curves were normalized to the corresponding value at $T = 0.2\ T_C$ and plotted as functions of the reduced temperature T/T_C. In the case of the 45° tilt junctions, I_C tends to saturate at lower temperatures. This behavior resembles more the dependence for traditional weak links characterized by low values of the ratio L/ξ_N (where L is the barrier thickness and ξ_N is the coherence length at $T = T_C$ in the normal barrier) and a barrier transparency that can be very low [15,16]. In the case of the 45° *twist*, an approximately linear increase of I_C is observed over a wide range of temperature down to 0.2 T_C. Such a behavior is typical of the HTS junctions that deviate from the ideal Josephson dependence [17]. The normal state resistances are slightly affected by the temperature both for the tilt and the twist case.

The quality of the junctions and the Josephson coupling have been also confirmed by the observation of reproducible Fraunhofer-like magnetic patterns. A typical dependence of the critical current I_C on an externally applied magnetic field (H) measured at $T = 4.2$ K is shown in Fig. 8, where I vs. V are reported as a function of H. Slight deviations manifested in the fact that I_C does not modulate down to zero. The pattern was symmetric around zero magnetic field, and in all samples the absolute maximum of I_C occurs at zero magnetic field [8,9].

The difference of this pattern from those of asymmetric in-plane 45° tilt bicrystal and biepitaxial junctions, in which the absolute I_C maximum is observed for $H \neq 0$, can be partly understood within the framework of a d-wave symmetry order parameter [1–3,8]. In fact, the presence of the absolute I_C

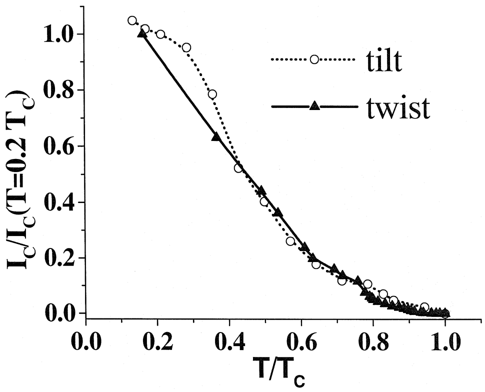

Fig. 7. Typical dependencies of the critical current I_C on the temperature T. I_C curves are normalized to the corresponding value at $T = 0.2\ T_C$ (80 μA for the tilt and 450 μA for the twist, respectively) and plotted as function of the reduced temperature T/T_C.

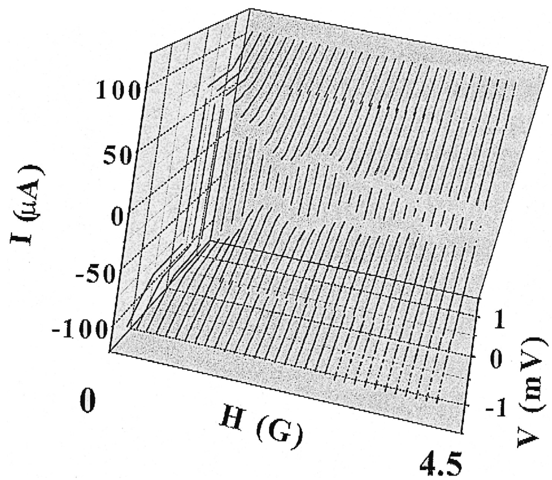

Fig. 8. $I-V$ curves are shown as a function of an externally applied magnetic field at $T = 4.2$ K. A typical Fraunhofer-like dependence of the critical current is evident.

maximum for $H \neq 0$ has been shown to be consistent with an interpretation based on $d_{x_2-y_2}$ wave symmetry and on GB faceting [8]. In Fig. 9 we illustrate the d-wave order parameter orientations for our junction configuration, and compare them with the ones in the asymmetric 45° tilt bicrystal, taking into account the intrinsic faceting. A fundamental difference is that the order parameter orientations do not produce an additional π phase shift along our junction independently of the details of the interface orientation in contrast with the 45° tilt asymmetric bicrystal junctions. On this basis we can argue that no unquantized magnetic flux would be expected in our junctions and low frequency $1/f$ noise could be smaller than in the asymmetric in plane 45° (001) tilt bicrystal and biepitaxial junctions.

The reproducible observation of Fiske steps gives information on the barrier of the *c*-axis 45° tilt and *twist* AGB. If we apply a Fiske mode analysis, the observed resonances roughly correspond to values of the barrier thickness normalized to the dielectric constant t_B/ε_r ranging from 0.015 nm to 0.05 nm [18,9]. These results are consistent with measurements on other types of GB junctions, characterized by low values of the critical current density [19–21] and show that the barrier can be dielectric in nature.

4. Atomically clean interfaces

Finally, we analyze the GB formation from the point of view of YBCO growth habits and show the modifications of the manufacturing process that can allow us to select a single type of atomically clean interface. On the basis of the HREM data, the only well-defined interfaces obtained in 45° or 90° *c*-axis tilt and *twist* boundaries are interfaces bound by the BP of one electrode. It would be highly desirable to employ the degrees of freedom of our fabrication process to select the formation of such an interface.

The expected growth of the GB with increasing film thickness is qualitatively sketched in Fig. 10a and b, respectively. The depicted evolution of the growing grains is based on established knowledge about the YBCO growth mechanism. One can see

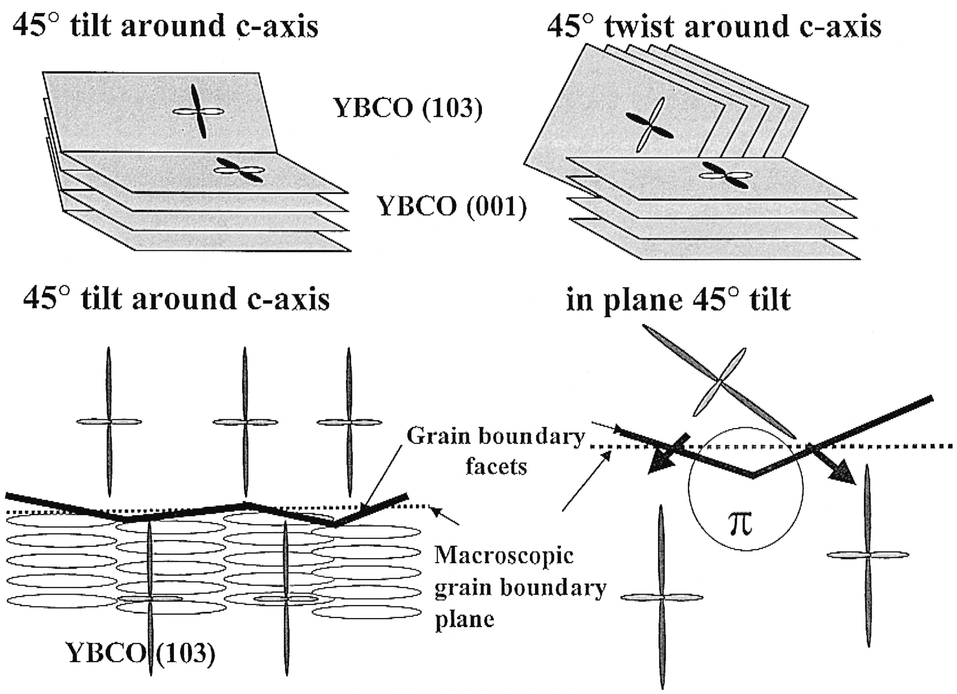

Fig. 9. The d-wave component expected in our junction configurations, compared with the one in the asymmetric in plane 45° tilt bicrystal, with the intrinsic faceting taken into account. The order parameter orientations do not produce an additional π phase shift along our junction in contrast with the 45° in-plane tilt junctions.

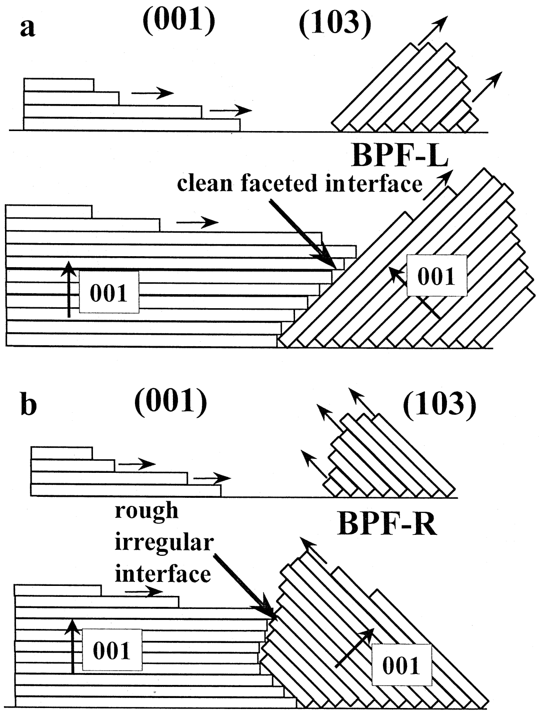

Fig. 10. (a) A schematic representation of the formation of a 45° tilt AGB with a BP of the (103) film as interface plane. This type of interface occurs when a BPF-L (103) oriented grain meets the (001) film. (b) When a BPF-R (103) grain meets the (001) film a rough irregular interface is formed.

that the situations shown in Fig. 10a and b correspond to the AGBs of the HREM images of Figs. 2 and 3, respectively. The contact of the *c*-axis grain with a basal plane face left (BPF-L) (103) grain leads to the formation of an almost perfect interface that might be suitable for the fabrication of homogeneous JJ. The contact of the *c*-axis grain with a basal plane face right (BPF-R) (103) grain leads instead to the formation of a rough irregular interface. These configurations are different not only because of the roughness which influences the uniformity of the junction but also for the microstructure, which could give rise to different transport properties.

In order to address the problem of removing one of the two (103) domains (that is, BPF-L and BPF-R), YBCO films were grown on exact and vicinal (110) STO surfaces and on vicinal (110) MgO substrate buffered with a STO (110) layer, in order to perform Reciprocal Space Mapping by X-ray diffraction [22]. The miscut angle of vicinal substrates was 3.5°, and the direction was (010). Symmetrical and asymmetrical maps were performed, with the scattering vector oriented in the vicinity of the [110] and of the [100]/[010] directions, respectively. Beside proving the excellent structural properties of our (103) YBCO films, the analyses showed that a total suppression (within experimental resolution) of one of the two domains is obtained with 3.5° miscut. It is deduced that a suitable alignment of the seed layer's edge with respect to the vicinal cut can allow us to orient all (103) grains with the BP in the GB direction, thus selecting the desired kind of interface. A sketch is

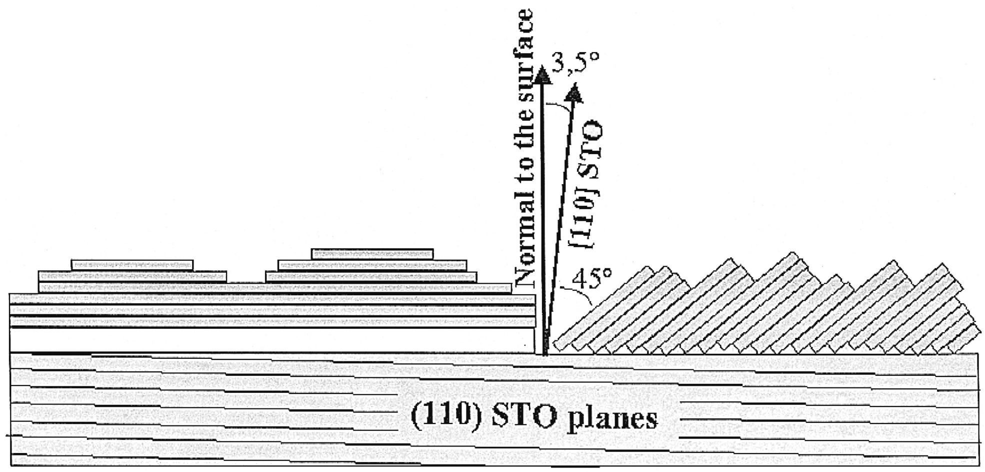

Fig. 11. A scheme of the tilt AGB on a vicinal substrate. A suitable alignment of the seed layer's edge with respect to the vicinal cut can allow to orient all (103) grains with the BP in the grain boundary direction, thus selecting the desired kind of interface.

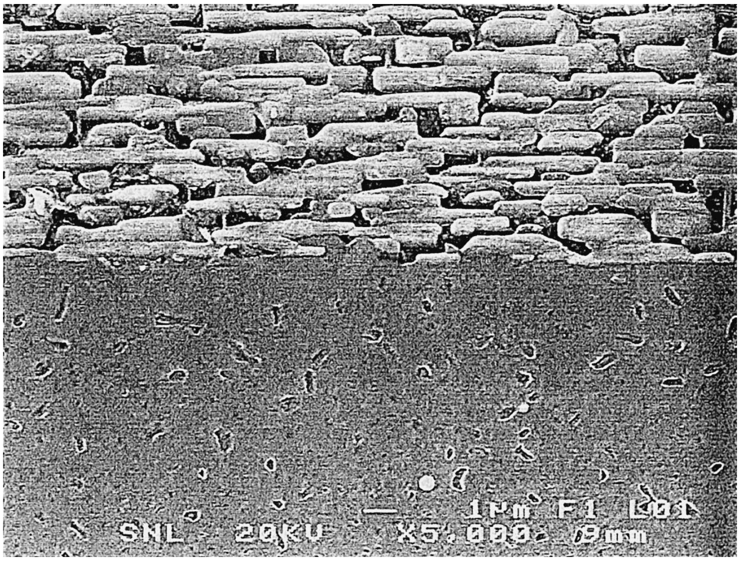

Fig. 12. SEM picture of tilt AGB obtained on a vicinal MgO substrate with a STO buffer layer.

shown in Fig. 11. A Scanning Electron Microscope (SEM) picture of a tilt AGB with the BP in the GB direction is shown in Fig. 12. The GB is obtained by removing part of the vicinal (110) STO seed layer from a (110) MgO substrate. The micrograph clearly shows a morphologically well defined interface between the needle-like (103) YBCO grains elongated along the (001) direction of the STO, and therefore parallel to the interface itself, and the (001) YBCO growth on the vicinal (110) MgO substrate. Investigations on the microstructural and transport properties of such 'engineered' boundaries are still in progress.

5. Conclusions

The Josephson properties and the microstructure of GB junctions characterized by a 45° relative misalignment of the *c*-axes (45° tilt and *twist*) have been investigated through transport and HREM measurements, respectively. We have employed a method to perform microstructural investigations by CS TEM on a JJ, whose properties have been previously measured, for a closer correlation between microstructure and transport properties.

The observed phenomenology gives evidence of profound differences with asymmetric in-plane 45° (001) tilt bicrystal and biepitaxial GB JJ. An explanation of these differences could be given in terms of the d-wave nature of the order parameter. The analysis indicates that the characteristics of the junctions described in this paper are promising for applications and fundamental studies. In particular we have shown that atomically clean interfaces can be reproducibly obtained by realizing our type of junction on vicinal substrates. Due to the type of GB, a low frequency $1/f$ noise lower than in the asymmetric in plane 45° (001) tilt bicrystal and biepitaxial junctions is expected.

Acknowledgements

This work was partially supported by the Istituto Nazionale di Fisica della Materia (INFM) under the project PRA JT3D 'High Temperature Superconductor Devices'. Part of this work has been performed within the framework of the Belgian IUAP 4/10. K.V. is a postdoctoral fellow of the Belgian FWO. The authors would like to thank Dr. J. Kirtley, Prof. A. Barone, Dr. E. Sarnelli and Dr. I. Bozovic for helpful discussions.

References

[1] C.C. Tsuei, J.R. Kirtley, C.C. Chi, L.S. Yu-Jahnes, A. Gupta, T. Shaw, J.Z. Sun, M.B. Ketchen, Phys. Rev. Lett. 73 (1994) 593.

[2] J.R. Kirtley, C.C. Tsuei, J.Z. Sun, C.C. Chi, L.S. Yu-Jahnes, A. Gupta, M. Rupp, M.B. Ketchen, Nature 373 (1995) 225.

[3] P. Chaudhari, S.-Y. Lin, Phys. Rev. Lett. 72 (1994) 1084.

[4] A. Braginski, in: H. Weinstock, R.W. Raltson (Eds.), The New Superconducting Electronics, Kluwer Academic Publishers, Dordrecht, 1993, pp. 89–105.

[5] J. Mannhart, P. Chaudhari, D. Dimos, C.C. Tsuei, T.M. McGuire, Phys. Rev. Lett. 61 (1988) 2476.

[6] D. Dimos, P. Chaudhari, J. Mannhart, Phys. Rev. B 41 (1990) 4038.

[7] K. Char, M.S. Colclough, S.M. Garrison, N. Newman, G. Zaharchuk, Appl. Phys. Lett. 59 (1991) 733.

[8] J. Mannhart, H. Hilgenkamp, B. Mayer, Ch. Gerber, J.R. Kirtley, K.A. Moler, M. Sigrist, Phys. Rev. Lett. 77 (1996) 2782.

[9] F. Tafuri, F.M. Miletto Granozio, F. Carillo, A. Di Chiara, K. Verbist, G. Van Tendeloo, Phys. Rev. B 59 (1999) 11523.

[10] K. Verbist, O. Lebedev, G. Van Tendeloo, F. Tafuri, F. Miletto Granozio, A. Di Chiara, Appl. Phys. Lett. 74 (1999) 1024.

[11] A. Di Chiara, F. Lombardi, F. Miletto Granozio, U. Scotti di Uccio, F. Tafuri, M. Valentino, IEEE Trans. Appl. Supercond. 7 (1997) 3327.

[12] A. Di Chiara, F. Lombardi, F. Miletto Granozio, G. Pepe, U. Scotti di Uccio, F. Tafuri, M. Valentino, J. Supercond. 9 (1996) 237.

[13] K. Verbist, F. Tafuri, F. Miletto Granozio, A. Di Chiara, G. Van Tendeloo, Proceedings of the 14th International Congress on Electron Microscopy, in: H.A. Calderon Benavides, M.J. Yacaman, Cancun, Mexico, 31 August–4 September 1998, Insitute of Physics, Bristol, Vol. II, p. 593.

[14] B.H. Moeckly, D.K. Lathorp, R.A. Buhrman, Phys. Rev. B 47 (1993) 400.

[15] K.K. Likharev, Rev. Mod. Phys. 51 (1979) 101.

[16] A. Barone, G. Games Paternò, Physics and Applications of the Josephson Effect, Wiley, New York, 1982.

[17] K.A. Delin, A.W. Kleinsasser, Supercond. Sci. Technol. 9 (1996) 227.

[18] F. Tafuri, B. Nadgorny, S. Shokhor, M. Gurvitch, F. Lombardi, F. Carillo, A. Di Chiara, E. Sarnelli, Phys. Rev. B 57 (1998) R14076.

[19] J. Mannhart, R. Gross, K. Hipler, R.P. Huebner, C.C. Tsuei, D. Dimos, P. Chaudhari, Science 245 (1989) 839.

[20] D. Winkler, Y.M. Zhang, P.A. Nilsson, E.A. Stepanstov, T. Claeson, Phys. Rev. Lett. 72 (1994) 1260.

[21] A. Beck, A. Stenzel, O.M. Froelich, R. Gerber, R. Gerdemann, L. Alff, B. Mayer, R. Gross, A. Marx, J.C. Villegier, H. Moriceau, IEEE Trans. Appl. Supercond. 5 (1995) 2192.

[22] U. Scotti di Uccio, F. Lombardi, F. Miletto Granozio, unpublished, 1999.